



# IMPROVEMENT OF METHOD FOR ESTIMATION OF THE RISK OF FRACTURE WITHIN THE THINNING ZONE ON WALLS OF MAIN PIPELINES

V.I. MAKHNENKO, E.A. VELIKOIVANENKO, G.F. ROZYNKA and N.I. PIVTORAK  
E.O. Paton Electric Welding Institute, NASU, Kiev, Ukraine

It is shown that application of the mathematical models, which are based on elimination of such assumptions as direct normals and a plane stress state, in deformation of the thinning zone in pipeline walls and presence of one local critical point with extreme (determinate) fracture conditions allows revealing the effect of peculiarities of an internal or external defect on a limiting pressure, as well as behaviour of a material within the deformation range from the beginning of plastic flow to fracture.

**Keywords:** welded pipelines, wall thinning, risk of fracture, improvement of estimation method, probability of fracture, Weibull law parameters, limiting pressure, external (internal) thinning defects

Numerous experimental tests and treatment of emergency fractures of modern gas pipelines show that fracture of metal within the zone of different thinnings of the pipe walls under conditions of intensive biaxial loading occurs at relatively low plastic strains acting in this region (up to 2.5–3.0 %). At such strains the main mechanism of fracture is cleavage, taking place under the effect of corresponding effective normal stresses at the fracture centre. This concept of fracture is also used in recommendations [1], where a criterion of the limiting state is permissible minimal thickness  $\delta_{min}$  of the pipe wall within the thinning zone with initial dimensions  $s_0$  along the pipe generating line and  $c_0$  along the circumference, which is determined as follows:

$$\delta_{min} \leq [\delta]R_j(s_0, c_0, D, [\delta]), \quad (j = s, c), \quad (1)$$

where  $[\delta]$  is the calculated permissible thickness of the pipe wall at a given point at the absence of thin-

ning; and  $R_j$  is the value depending upon  $[\delta]$ ,  $s_0$ ,  $c_0$  and pipe diameter  $D$  [1] ( $0.2 \leq R_j < 1.0$ ).

These recommendations [1] have been well verified experimentally and are accepted as an approximate, rather conservative approach to estimation of acceptability of thinning defects. In this case, ignored are such factors as external or internal thinning defect, defect geometry within dimensions  $s_0$ ,  $c_0$ ,  $(\delta - \delta_{min}) = a$ , properties of a material in the form of deformation resistance in a region above the yield stress and before fracture due to cleavage at critical strains of about 2.5–3.0 %, which are approximately an order of magnitude higher than those outside thinning, at which the value of  $[\delta]$  is determined at a stage of pipeline design.

The question of stochasticity of a number of geometric data with regard to thinnings, as well as of mechanical properties of a material within the thinning zone after a long-time operation often arises in practical estimations of the risk of fracture.

The task of this study was to develop the calculation algorithms to be used to answer the above questions at reasonable costs while investigating behaviour of different local thinnings on pipelines under loading conditions.

For this, it was necessary to choose a model of deformation of the pipe wall, not relating it to the main hypotheses of thin-walled shells (direct normal and plane stress state), as well as a model of fracture of a material at relatively low strains, where stochasticity of initiation of fracture has not yet been forgotten due to a developed plastic flow

The deformation model is based on the 3D mathematical description in the cylindrical system of coordinates  $r, z, \beta$  of the deformed region of the pipeline wall (Figure 1) delineated by coordinate planes  $z = \text{const}$ ,  $\beta = \text{const}$  with an internal or external defect, the surface of which is set by the following equation:

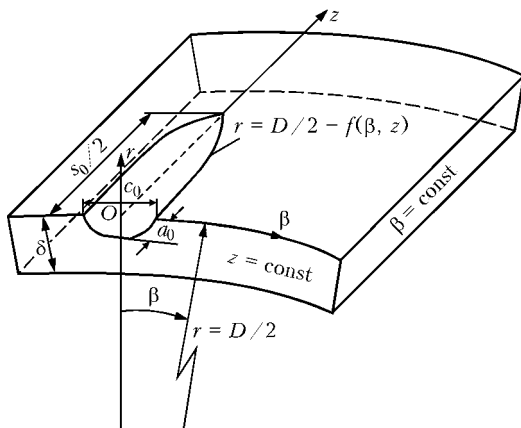


Figure 1. Schematic of the region of pipeline wall (region V) cut out by coordinate planes  $z = \text{const}$  and  $\beta = \text{const}$ , and thinning defect with dimensions  $a$ ,  $s_0$  and  $c_0$



$$r = \frac{D}{2} - f(\beta, z). \tag{2}$$

$$d\varepsilon_{ij}^p = d\lambda(\sigma_{ij} - \sigma). \tag{7}$$

The boundary conditions set at the boundary planes (Figure 1) and surface of the defect correspond to those set for the entire pipe with no allowance for thinning, which is quite acceptable at sufficiently local thinning dimensions  $s_0$  and  $c_0$ .

Classical relationships between components of strain tensor  $\varepsilon_{ij}$  and displacement vector  $U_i$  in the context of the theory of low elasto-plastic strains [2] hold inside region  $V$  limited by the above boundary planes and surface of the defect, i.e.

$$\begin{aligned} \varepsilon_{rr} &= \frac{\partial U_r}{\partial r}, \quad \varepsilon_{\beta\beta} = \frac{U_r}{r} + \frac{\partial U_\beta}{r\partial\beta}, \quad \varepsilon_{zz} = \frac{\partial U_z}{\partial z}, \\ 2\varepsilon_{r\beta} &= \frac{1}{r} \frac{\partial U_r}{\partial\beta} + r \frac{\partial}{\partial r} \left( \frac{U_\beta}{r} \right), \quad 2\varepsilon_{z\beta} = \frac{\partial U_\beta}{\partial z} + \frac{\partial U_z}{r\partial\beta}, \\ 2\varepsilon_{rz} &= \frac{\partial U_r}{\partial z} + \frac{\partial U_z}{\partial r}. \end{aligned} \tag{3}$$

Relationships (3) are also valid for components of strain increment tensor  $\Delta\varepsilon_{ij}$  and displacement increment vector  $\Delta U_i$  used at plastic deformation in the context of the theory of elasto-plastic flow.

Components of stress tensor  $\sigma_{ij}$  inside region  $V$  meet equilibrium equations, i.e.

$$\begin{aligned} \frac{\partial}{\partial r} (r\sigma_{rr}) + \frac{1}{r} \frac{\partial \sigma_{r\beta}}{\partial\beta} + \frac{\partial \sigma_{rz}}{\partial z} &= \sigma_{\beta\beta}, \\ \frac{\partial}{\partial r} (r\sigma_{r\beta}) + \frac{1}{r} \frac{\partial \sigma_{\beta\beta}}{\partial\beta} + \frac{\partial \sigma_{\beta z}}{\partial z} &= 0, \\ \frac{\partial}{\partial r} (r\sigma_{rz}) + \frac{1}{r} \frac{\partial \sigma_{z\beta}}{\partial\beta} + \frac{\partial \sigma_{zz}}{\partial z} &= 0. \end{aligned} \tag{4}$$

Relation between the stress tensor and displacement increment within the framework of the theory of elasto-plastic flow can be written down as follows:

$$d\varepsilon_{ij} = d \left[ \left( \frac{\sigma_{ij} - \sigma}{2G} \right) + K\sigma \right] + d\lambda(\sigma_{ij} - \sigma), \tag{5}$$

$(i, j = r, z, \beta),$

where  $d\lambda$  is the scalar coordinate function, which is determined by the Mises yield condition with isotropic hardening, i.e.

$$\begin{aligned} d\lambda &= 0, \text{ if } f = \sigma_{\text{eq}}^2 - \sigma_s^2(\omega) < 0, \\ &\text{or } f = 0, \text{ but } df < 0, \\ d\lambda &> 0, \text{ if } f = 0 \text{ and } df > 0. \end{aligned} \tag{6}$$

Condition  $f > 0$  is inadmissible.

Here  $\sigma = 1/3(\sigma_{rr} + \sigma_{\beta\beta} + \sigma_{zz})$ ;  $\sigma_{\text{eq}}$  is the equivalent stress for tensor  $\sigma_{ij}$ ;  $\sigma_s(\omega)$  are the deformation stresses for a given material depending upon strain hardening parameter  $\omega$ ;  $\omega = \int d\varepsilon_{\text{eq}}^p$  is the Odquist parameter;  $d\varepsilon_{\text{eq}}^p$  is the increment of equivalent plastic strain for tensor  $\varepsilon_{ij}^p$ ; and

To implement model (2) through (4), this study used the method of step-by-step tracing of loading of volume  $V$  by a growing external load (e.g. internal pressure  $\bar{P}$ ). Yield condition (6) was allowed for at each tracing step by the iteration method [3].

The fracture model is based on an idea of probable fracture due to cleavage within the thinning zone (volume  $V$ ), where maximal main stresses  $\sigma_1$  in this volume meet condition

$$p = 1 - \exp \left[ - \int_V \left( \frac{\sigma_1 - A}{B} \right)^\eta \frac{dV}{V_0} \right], \quad \sigma_1 > A. \tag{8}$$

Integration was carried out only with respect to elementary volumes  $\Delta V$ , for which  $\sigma_1 > A$ ;  $A$ ,  $B$  and  $\eta$  are the parameters of the Weibull three-parameter distribution law; and  $V_0$  is the structural parameter of a given steel at brittle fracture  $V_0^{\text{br}} \sim (0.05 \text{ mm})^3$  at the crack apex and at tough fracture  $\sim h^3$ , where  $h$  is the characteristic size of finite elements providing a sufficiently accurate numerical solution for  $\sigma_1$  by deformation models (2) through (7) within the thinning zone. In other words, the value of  $V_0$  can be assumed to be equal to  $\Delta V$  in breaking down of volume  $V$  (Figure 1) into finite elements. The rest of the parameters in model (8) are determined by comparing the calculation by models (2) through (7) with the corresponding experimental data. Our investigations show that the recommendations of study [1], based on numerous experiments, i.e. expression (1), can be used as a first approximation, assuming that fracture probability  $p$  is not in excess of 0.05.

Certain simplifications can also be made in fracture model (8), allowing for the presence of extreme planes  $\beta = \text{const}$  and  $z = \text{const}$ , where normal stresses  $\sigma_{\beta\beta}$  or  $\sigma_{zz}$  are close to  $\sigma_1$ , and a layer corresponding to  $\beta = \text{const}$  with thickness  $\Delta\beta R$ , or  $z = \text{const}$  with thickness  $\Delta z$  can be assumed to be an integration volume in (8). Allowing for this consideration based on the corresponding experimental data, e.g. [1], and following the principle of the maximum likelihood (minimising the discrepancy by probability  $p$ ) in variation of thinning sizes ( $s_0, \delta_{\text{min}}$ ) parameters  $A, B$  and  $\eta$  can be determined at given geometric dimensions and mechanical properties of the pipeline material. The outcome of this approach shows that the sufficiently good results can be obtained at  $\eta = 4.0$  and  $A = \frac{\sigma_t + \sigma_y}{2}$  ( $\sigma_t$  and  $\sigma_y$  are the tensile strength and yield stress of the material, respectively, in the thinning zone).

The value of  $B$  at the above recommendations with respect to  $V_0$  can readily be checked on the basis of model (8). As a result, the data on  $A, B$  and  $\eta$  for a specific steel, as well as sizes of different shapes of thinning being known, the probability of fracture can be calculated for different geometric parameters of a

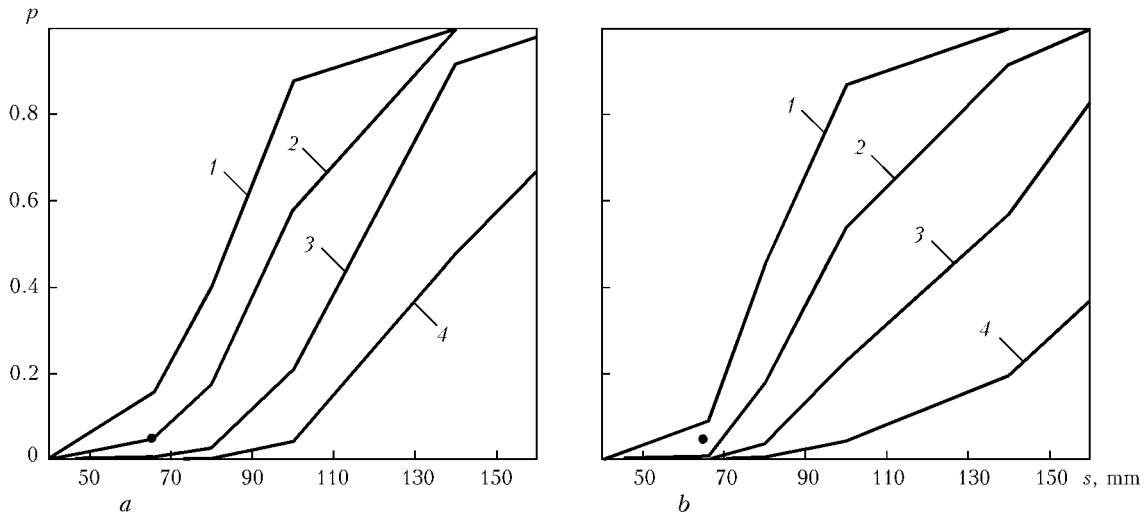


**Figure 2.** Probability of fracture in the defect (wall thinning) zone with  $a = 14$  mm and  $c = 40$  mm, depending on  $s$  and  $\bar{P}$  for external (a) and internal (b) defect in the  $1420 \times 20$  mm pipe at  $\sigma_y = 440$  MPa,  $A = 500$  MPa and  $B = 420$  MPa (● – experimental data): 1 –  $\bar{P} = 10$ ; 2 – 9; 3 – 8; 4 – 7 MPa

pipeline and internal pressure  $\bar{P}$  on the basis of models (2) through (8).

Figures 2 and 3 show the results for the 17G1S steel pipeline with  $D \times \delta = 1420 \times 20$  mm at the presence of a surface wall thinning defect, the shape of which can be described depending upon coordinates  $z, r, \beta$  by the following second-order equation:

$$\left(\frac{R_q - r}{a}\right)^2 + \left(\frac{2z}{s_0}\right)^2 + \left(\frac{D\beta}{c_0}\right)^2 = 1, \quad (9)$$

where  $R_q = D/2$  for the external defect and  $R_q = (D - 2\delta)/2$  for the internal defect; and  $a, s_0$  and  $c_0$  are the dimensions of the defect with symmetry axes  $z = 0$  and  $\beta = 0$ .

Noteworthy among the data in Figures 2 and 3 is a differing load-carrying capacity of the external and internal defects, i.e. resistance to the internal pressure, as well as a substantial effect of the defect depth (value  $a$ ).

As seen from Figures 2 and 3, the external defect is characterised by a lower resistance to the internal

pressure than the internal one. However, this difference is high in the zone of high fracture probabilities ( $p > 0.1$ ), which is of low interest to practice. Therefore, the absence of differentiation of thinning defects between the internal or external ones in study [1] is reasonably justified, based on the data on the external thinning defect in pipeline walls. Nevertheless, this fact should be kept in mind.

The data in Figure 3 for shallower defects ( $a = 10$  mm), compared with the data in Figure 2 for deep defects ( $a = 14$  mm), are characterised by a lower restriction of deformation, lower stresses and, accordingly, lower failure probabilities, this being determined not only by lower stresses, but also by a value of  $B$  at constant  $A = 500$  MPa and  $\eta = 4.0$ . So, based on the above choice according to the given recommendations [1],  $B = 420$  MPa for  $a = 14$  mm in Figure 2, and  $B = 830$  MPa for  $a = 10$  mm.

Of certain interest are the data shown in Figures 4 and 5, which illustrate the effect of dimension  $c$  for a deep thinning with  $a = 14$  mm at constant  $s = 66$  mm on the probability of fracture, according to the model

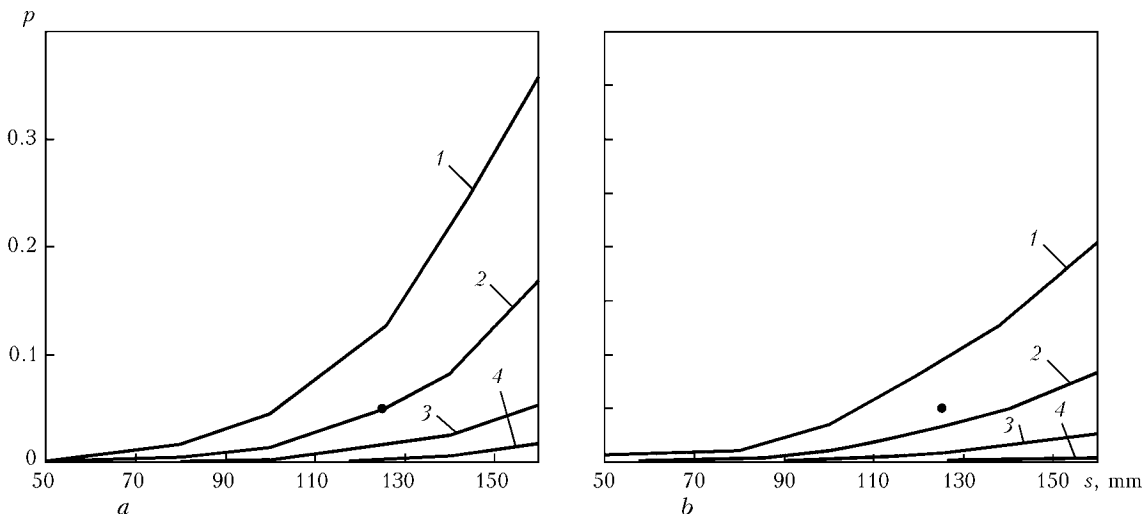


**Figure 3.** Probability of fracture in the defect (wall thinning) zone with  $a = 10$  mm and  $B = 830$  MPa depending on  $s$  and  $\bar{P}$  for external (a) and internal (b) location of the defect (the rest of designations are the same as in Figure 2)

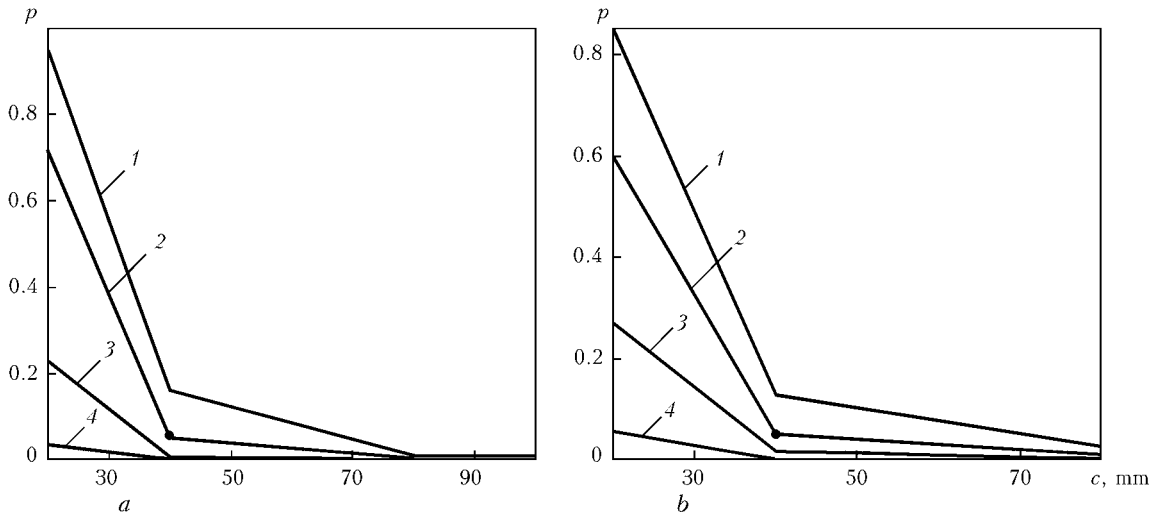


**Figure 4.** Effect of defect width  $c$  on fracture probability  $p$  in a pipe measuring  $1420 \times 20$  mm with  $\sigma_y = 440$  MPa for different  $\bar{P}$  and constant  $s = 66$  mm at the defect depth:  $a - a = 14$  mm,  $B = 420$  MPa;  $b - a = 10$  mm,  $B = 830$  MPa;  $1 - \bar{P} = 10$ ;  $2 - 9$ ;  $3 - 8$ ;  $4 - 7$  MPa

employed. These data on a relatively low effect of the  $c$  value of the thinning defect at sufficiently high  $s$  and  $c$  on the fracture resistance are in good agreement with the experimental data given in [1] and other studies. The new data, compared with this situation, are those of the type shown in Figure 4 at  $c < 20$  mm (comparable with thickness of the pipe wall). In this case, the groove-like thinning defect is close to a crack, and the concentration of stresses grows accordingly, this affecting the value of the failure probability.

When estimating the load-carrying capacity of thinning defects, it is important to know the distribution of load in metal in plastic deformation that leads to a decrease in the concentration of stresses.

Figure 6,  $a$  shows the data on the effect of ratio  $\sigma_t/\sigma_y$  at constant  $1/2(\sigma_t + \sigma_y) = A = 500$  MPa on limiting pressure  $\bar{P}_{limit}$  in a pipe under consideration, measuring  $D \times \delta = 1420 \times 20$  mm, at fracture probability  $p = 0.05$  and presence of a thinning defect with depth  $a = 10$  mm, extended along axis  $s = 140$  mm and along circumference  $c = 40$  mm.

Depending upon Odquist hardening parameter  $\omega$  (6), the use was made of the power law of hardening of a material in deformation:

$$\sigma_s^{(\omega)} = \sigma_y \left( 1 + \frac{\omega}{\varepsilon_0} \right)^m, \text{ where } \varepsilon_0 = \frac{\sigma_y}{E}, \quad m = 0.14.$$

Ratio  $\sigma_t/\sigma_y$  was varied in a range with  $\sigma_t = 350 - 440$  MPa at  $A = 500$  MPa. For pipe steels, such a wide range of variations in  $\sigma_t/\sigma_y$  is unlikely. However, it allows the effect of material deformation conditions beyond the bounds of elasticity on the limiting state within the thinning defect zone to be demonstrated more clearly.

It can be seen that limiting pressure  $\bar{P}_{limit}$  grows with increase in  $\sigma_t/\sigma_y$  at constant  $A = 1/2(\sigma_t + \sigma_y)$ . This effect is attributable to the character of redistribution of load within the defect zone depending upon the level of material yield stress  $\sigma_y$ . The lower the value of  $\sigma_y$ , the more uniform is the distribution of normal stresses within the defect zone under loading, this eventually leading to decrease in probability  $p$ .

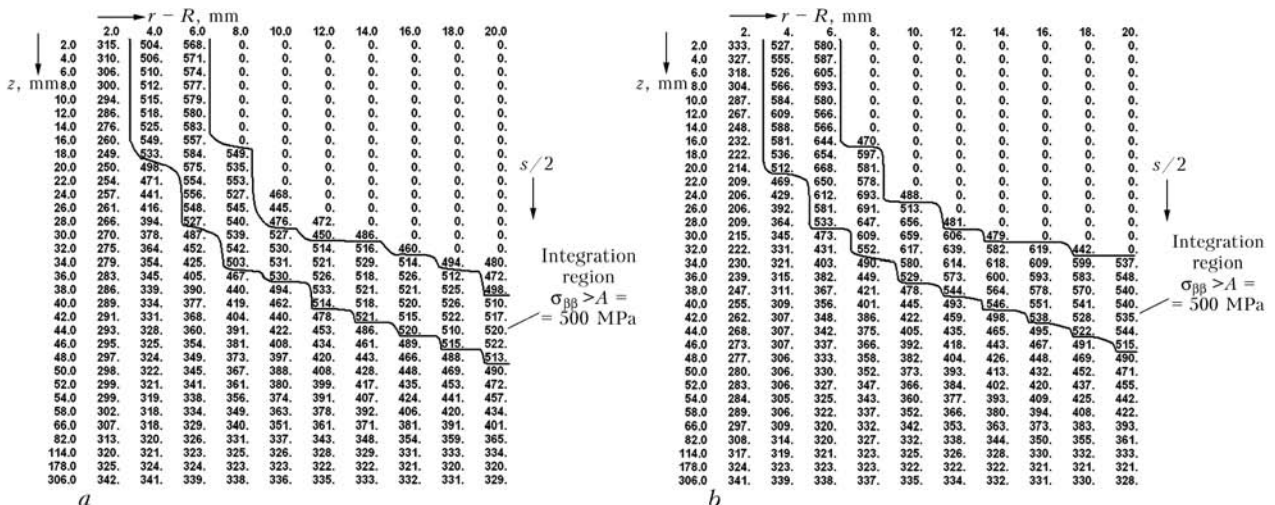


**Figure 5.** Distribution of circumferential stresses  $\sigma_{\beta\beta}$  in symmetry plane  $\beta = \beta_{cr}$  at  $\bar{P}_{limit} = 10$  MPa,  $\sigma_y = 440$  MPa,  $a = 14$  mm,  $s = 66$  mm,  $c = 40$  (a) and 20 (b) mm

